Unprecedented Retreat of Columbia Glacier Relative to the Last Millennium

By

Zoe Kilmer

An Undergraduate Thesis Submitted to

Oregon State University

In partial fulfillment of
the requirements for the
degree of

Baccalaureate of Science in BioResource Research,
Water Resources

March 1st, 2017

APPROVED:

_____	_____
Anders Carlson, College of Earth Ocean and Atmospheric Science	3/1/17
_____	_____
Joseph Stoner, College of Earth, Ocean, and Atmospheric Science	3/1/17
_____	_____
Katharine G. Field, BRR Director	3/1/17

ABSTRACT

Columbia Glacier, Alaska's most rapidly retreating body of ice, provides a compelling insight into the fragile state of tidewater glaciers worldwide. Catastrophic retreat of the glacier's terminal ice margin began in 1978 when contact was lost with its stabilizing terminal moraine shoal. Since this time, Columbia Glacier has lost ~20 km in length and ~100 km^2 of previously ice covered area. Here we used magnetic and geochemical variability in a proximal marine sediment record to analyze the magnitude of recent retreat in relation to a millennial timescale, and suggest potential driving mechanisms of glacier destabilization. At ~0.9 kya, a distinct shift in magnetic minerology coincides with a change in sediment geochemistry. This sediment provenance change records the glacier's most recent substantial advance, in which it crossed the Contact Fault and began eroding mafic lithologies distinctive of the region's basalt and granitic intrusions. The marine record depicts Columbia Glacier remaining stable in this extended position south of the Contact Fault until the most recent rapid mass loss ensued, making recent retreat of Columbia Glacier unprecedented since ~0.9kya. Analyzing the driving mechanisms behind this anomalous retreat proved difficult due to tidewater glaciers' complex relationship with non-climatic forcings. However, we found that a 1.2°C temperature anomaly occurred during times of Columbia Glacier destabilization in both modern day retreat, and the prehistorical retreat that occurred ~0.9kya. Using a glacial destabilization model simulation, we further concluded that a 1.1±.2°C temperature increase induced Columbia Glacier retreat. Thus, we conclude that the initial detachment of Columbia Glacier from its marine shoal, an event that triggered catastrophic retreat by a positive feedback system of calving and resupplying ice flow, was likely the result of a 1.2°C surface air temperature increase over a 70-year period.

1. INTRODUCTION

Columbia Glacier, Alaska's most rapidly retreating body of ice, provides a compelling insight into the fragile state of tidewater glaciers worldwide. The glacier originates at 3500m in the Chugach Mountain range of Alaska's south central Prince William Sound (PWS), and extends fully grounded to sea level, where it flows into Columbia Bay (O'Neel et al., 2005). Climate of the region is driven by a moderate coastal temperature profile and locality in relation to the Aleutian Low pressure feature. Storm systems propagate into the region from the Aleutian Low, carrying saturated air masses, and deposit immense snowfall when incident of the Chugach Mountain range, as a result of orographic uplift. This winter accumulation is coupled with extensive summer melting by above freezing summer temperatures resulting from its temperate conditions. Columbia Glacier is thus an exemplary isothermal, meltwater dominated glacier in which mass balance is driven by high rates of accumulation and melting, resulting in anomalous ice velocities by basal sliding mechanisms (Post et al., 1976). The high accumulation rate regime is evident in the complex, dendritic array of four tributary ice flows conjoining into one southerly flowing main trunk that, today, covers an area of ~1000 km^2 over a length of 47 km. Columbia Glacier has a long history of remaining impeccably stable, with only short lived advances and retreats since its Little Ice Age Maximum extent was reached in 1800 A.D (Barclay, Wiles, and Calkin, 2009).

1.1 Recent Retreat

An immanent shift out of this stable equilibrium state culminated in 1978 when accumulation season readvances no longer sufficiently filled embayments that left the

glaciers terminal ice margin detached from its moraine shoal (Molina, 2008). This moraine shoal, the submarine portion of the glacier's terminal moraine, increased static stability of the terminal ice margin by reducing freshwater buoyancy forces and insulating the ice from contact with the comparatively warm, erosive seawater. Without the stabilizing effects of its moraine shoal, the glacier began rapidly losing mass by coupled rates of calving and resupplying ice flow, resulting in further retreat into deeper water (Post, 2011). The overall rate of glacial retreat has exponentially increased in the last 35 years as a result of this positive feedback mechanism. In total, ~20km of length and 100km^2 of ice covered area from the pre retreat length of ~67 km and area of 1100km^2 have currently been lost (McNabb and Hock, 2014). Today, retreat remains fully self-sustained, with discharge flux greatly exceeding the mass balance flux, and is predicted, if climatic forcings remain constant, to continue until 2020 when a new stable terminus position is reached (Colgan et. al., 2012).

1.2 Impacts of Recent Retreat

As the largest glacier in PWS, the recent retreat of Columbia Glacier has a profound impact on the economical and biological success of the region's ecosystem. The region serves many diverse industries, including globally profitable commercial fisheries, the primary marine highway of vessels exporting crude oil from the southern terminus of the Trans-Alaska Pipeline, and coastal and terrestrial tourism attractions. PWS is also home to a robust biological food web providing spawning and rearing grounds to species migrating from across the world's oceans (Etherington., et al 2009). The first order influence of hydrological factors in this predominately glaciated basin, the backbone to the multitude of

resources PWS sustains, is the glacial surface energy balance and resultant glacial freshwater discharge (Hill et al., 2009).

Glacier-fed streams exhibit modified physical characteristics in comparison to those influenced by a precipitation based regime (O'Neel et al., 2015). The high annual volume discharge, drought resistant, cold and turbidic characteristics of these streams result in highly specialized endemic taxa and are vital breeding and rearing locations for summer spawning species (Jannson et al. 2013). For example, glacier-fed streams are essential for the vitality of the five Pacific Salmon species, which are responsible for a harvest producing annually over 500 million dollars in profit to the PWS economy (Alaska Fish and Game). Freshwater streams are deposited into PWS and become the first order forcing of the Alaska Coastal Current (ACC), the region's primary near shore ocean current. Freshwater drives the degree of water column stratification and barotropic gradient (Hill et al., 2009). The resultant mixed layer depth both determines nutrient availability to autotrophic organisms that support higher trophic level production, and drives the seasonal variation of speed and direction of geostrophic flow within the sound (Musgrave, 2013).

On a global scale, retreating tidewater glaciers are the dominant component of global sea level rise, based on their ability to transfer large quantities of mass via iceberg calving. Thus, as the fastest retreating tidewater glacier in Alaska, Columbia Glacier is the single largest contributor to sea level rise of all Alaskan glaciers. From 1995 to 2001, it released 7.3 km^3a^{-1} of freshwater into Columbia Bay, equivalent to 0.06% of the total sea level rise observed worldwide between 2003 and 2007 (Berthier, 2010). Understanding the susceptibility of these tidewater glaciers to large-scale retreat in a changing climatic state gives vital insight into analyzing the downstream feedbacks altering physical,

chemical, and biological systems and determining the degree of forthcoming global sea level rise.

1.3 Tidewater Glacier Cycle

Tidewater glaciers have a particularly complex relationship with climate change due to their sensitivity to non-climatic forcings (Post, 2011). Internal ice dynamics such as ice flow acceleration, calving events, respective drainage basin, and fjord geometry and bathymetry are primary drivers of tidewater glaciers advance and retreat. These controls on ice dynamics further complicate the understanding of underlying driving forces by creating asynchronous behavior of glaciers in relatively close proximity. The shoreline of Prince William Sound, for example, is home to tidewater glaciers that are currently within different stages of the tidewater glacier cycle (Post, O'Neil, Motyka, 2011). This widely accepted model depicts the cyclic nature of tidewater glaciers, in which a slow, stable advance occurs on the order of millennial time scales followed by rapid disintegration occurring in less than a century. In a short, decadal to centennial time scale, this suggests why in Prince William Sound alone Columbia Glacier is undergoing rapid retreat, Harvard Glacier is slowly advancing, and Shoup Glacier is in post retreat stability (Meier 1985). Why then in today's rapidly changing climatic state, are tidewater glaciers predominantly in a stage of retreat? Statistically speaking, if no climatic influences were at play, tidewater glaciers worldwide would be predominantly advancing, as the advance phases significantly outlasts the retreat phase. Of the 51 tidewater glaciers that currently exist in Alaska, 6 are experiencing rapid retreat, 30 have begun slowly retreating since 1999, 11 have remained stable since 1999, and a total of 6 are currently advancing (Molina., 2008; McNabb and

Hock, 2014). Growing evidence points to marine terminating glacier instability in various other regions characterized by isothermal glacial regimes. The Northern and Southern Patagonian Ice fields, the largest temperate ice masses in the Southern Hemisphere, have been losing ice volume on a centennial to decadal time scale due to rapid changes in marine terminating outlet glaciers (Sakakibara and Sugiyama, 2014). Furthermore, the leading consensus on glacial thinning of the Greenlandic Ice Sheet, is perturbations at the ice front of marine terminating glaciers (Staneo et al., 2013). There is thus a clear need for reevaluating what effects climatic controls have on the ice dynamics of these glacial systems.

A critical step in evaluating this climatic control is determining whether anomalous recent retreat is in comparison to the past, and resolving what climatic states of the past produced similar glacial dynamics. This is rather difficult, as glaciers typically erase proxy material of past retreats with each subsequent advance. Furthermore, it is not until retreat ensues that proxies overrun during ice advance can be used for evaluating the past. Here, we instead take a novel approach to these issues, using the geographic locality of Columbia Glacier and resultant sediment.

1.4 Geologic Setting

The PWS sound is geologically composed of the Chugach and Prince William Sound terranes which were episodically accreted to the western margin of North America as a result of complex plate interactions beginning in the early Mesozoic. The accretionary prism is made up of two belts of chronologically and lithologically distinct bedrock groups that young in a seaward direction and are divided by the Contact Fault (Winkler, 2000).. In

the PWS the Contact Fault is well exposed by thrust fault surface exposure and signs of deformations. The inboard (northern) Valdez group, one of the three accretionary sequences of the Chugach terrane, was deposited between 70 and 75 Mya. This belt is made up of flysch and basalt assemblages that underwent an intensive metamorphic event at ~50 mya that resulted in greenschist facies (Winkler, 2000). The accretionary complex is thus generally made up of deformed metasedimentary and metavolcanic rocks (Miller, 2014). The outboard (southern) Orca group, the sole accretionary prism of the Prince William Sound terrane, formed between 60-50 Mya. This prism is made up of ~80% flysch sequences similar to Valdez Group flysch sequences, and ~20% of Paleocene intruded ophiolites of mafic and ultramafic basalts and granites. The Orca Group was also affected by the regional metamorphic event at ~50 Mya; however, grades are less so than the Valdez Group (Winkler, 2000). In general, the Orca Group is distinguished as sedimentary rocks with local outcrops of mafic and ultramafic basalts and granitic intrusions (Miller, 2014).

The Contact Fault bisects the basal surface of Columbia Glacier ~16km north of the glacier's 1978 equilibrium position (Fig. 2). As Columbia Glacier advances and retreats, it crosses the fault boundary and results in basal erosion of bedrock of different lithological composition. At its 1980 stable equilibrium position, Columbia Glacier resided to the south of the Contact Fault, eroding both Orca Group sandstones and intruded mafic basalts at its terminal ice margin. However, in its modern day retreated position, the Columbia Glacier now resides to the north of the Contact Fault, and thus erodes Valdez Group metasedimentary and metavolcanic material at its terminal ice margin. By analyzing the variation in bedrock type produced over time, the position of Columbia Glacier in relationship to the Contact Fault can be determined.

1.5 Prior State of Knowledge

In 2004, Oregon State faculty members aboard the *R/V Ewing* retrieved marine jumbo piston and trigger core EW0408-95(JC/TC) and multi core EW0408-95(MC) (60.66°N, 147.71°W, 744 m water depth), located ~40 km from the 1978 terminus position of Columbia Glacier. Initial measurements were obtained from sediment u-channels, including the down core magnetic grain size profile (kARM/k), a well-known proxy determined by the ratio of anhysteretic remnant magnetization (kARM) and bulk sediment susceptibility (k). Within the record existed two pronounce phases in the magnetic regime divided by a sudden shift between the two. Greater depths within the core were characterized with a weakly magnetic, coarse grained material (low kARM/k) and relatively high variability, shifting to a strongly magnetic, fine grained material (high kARM/k) with low variability as the core decreases in depth and age. This previously determined down core magnetic profile indeed distinguished a drastic change in the proxy for magnetic grain size. Yet, the shift in magnetics lacked a definite correlation to the activity of Columbia Glacier. Nor was the sediment in the core distinguished as being of Columbia Glacier origin.

Here we couple this magnetic regime shift with sediment geochemical variability in the proximal marine core and bulk terminal moraine sediment samples to analyze the magnitude of recent Columbia Glacier retreat in relation to a millennial timescale of glacial dynamics, and further suggest potential driving mechanisms of Columbia Glacier destabilization.

2. METHODS

2.1 Marine Core Chronology

To further constrict marine core chronology, originally established by Leah Ziegler, five additional mixed benthic radiocarbon measurements were obtained from the >63µm sand fraction at various depths within EW0408-95JC (Tab. 2). In addition, one benthic/planktonic pair was collected at 780 cm downcore depth where sufficient planktonic foraminifera tests existed. This sample was utilized to identify the surface to deep-water age DR of 340 +/- years, which combined with the regional surface ocean DR of 470 +/- 80 years (McNeely et al., 2006; Davies-Walczak et al., 2014) gave a total benthic DR of 810 +/- 100 years. This value was then utilized in correcting raw benthic radiocarbon ages to relevant calendar ages. Predominant benthic foraminifera included *Uvigerina peregrina, Bolivina alata,* and *Cibicides lobatulus,* predominant planktonic foraminifera included *Neogloboquadrina pachyderma* and *Globigerina bulloides.* Radiocarbon measurements were collected by Maureen Davies-Walczak at the Australian National University following techniques in (Davies-Walczak et al., 2014). Raw radiocarbon ages were calibrated to calendar years using IntCal13 and integrated with Pb^{210} and Cs^{137} data available on EW0408-95MC to create an age model using Bchron.

2.2 X-Ray Florescence Core Scanning

Marine core geochemistry was determined using Oregon State University's ITRAX X-Ray Fluorescence core scanner. Measurements were taken at 1mm resolution on EW0408-95 JC, and 0.2mm resolution on EW0408-95 TC and EW0408-94MC. The relative concentrations of the following elements were collected: Ar, Si, K, Ca, Fe, Ti, Sr, P, S, Cl, Al, V,

Cr, Mn, Cu, Zn, Ni, Br, Ba, La, Ce, Rb, Y, Pr, and Nd. Based on the geologic makeup of the differing bed rock types between the north and south sides of the Contact Fault, we utilized the ratios Si/Ca and Si/Fe to depict the transition when the glacier crossed from residing north of the Contact Fault to residing south of it. Ca and Fe were normalized to Si, as both sides of the fault contain marine sedimentary bedrock high in sandstone composition. Down core records were smoothed to a decadal average, as a < 1 cm yr^{-1} sedimentation rate within the region gave annual to sub-annual resolution prior to smoothing.

2.3 Bulk Sediment Sample Collection

Marine core sediment provenance was determined by collection of 12 sediment samples from terminal moraines and glacial fed streams in the PWS region (Tab. 1, Fig. 1). We then chose to obtain and compare the geochemical and magnetic characteristics of sediment collected from the terminal moraine of Columbia Glacier versus that of sediment collected from the terminal moraine of Shoupe Glacier. These samples were obtained via transportation from the Port of Valdez aboard the small craft vessel *Alycon.* Shoupe Glacier's terminal moraine at its most recent maximum extent (1750 C.E.) is located north of the Contact Fault, while Columbia Glacier terminal moraine at its most recent maximum extent (1980 C.E.) is located south of the Contact Fault (Fig. 2). Shoupe Glacier's terminal moraine was chosen of the 12 samples obtained for comparison to Columbia Glacier based on its distance away from anthropogenic influences, increasing sample integrity, its locality on bedrock type resembling that on which Columbia Glacier resides, in a modern day retreat position north of the Contact Fault, and its end member source in our marine core site based on regional oceanographic dynamics.

2.4 Bulk Sediment Geochemical Analyses

Relative geochemical elemental profiles of sediment collected from the Columbia Glacier terminal moraine and Shoupe Glacier terminal moraine were obtained by inductively coupled plasma atomic emission spectrometry (ICP-AES). Approximately 0.25 grams of sediment from each terminal moraine were dissolved in 10 mL HF and 1mL of HNO_3. Samples were heated to ~100 C° to evaporate the HF and HNO_3. The now liquid samples were then transferred to centrifuge tubes and normalized to 10 mL of total volume with Millipore H_2O. Centrifuge tubes were then sent to the University of Colorado, Boulder, for Quartz purity testing by ICP-AES. In total, the following elements were analyzed for their relative concentration in each sample: Be, Al, Fe, Ti, Ca, K, Na, Mg, Sr, Si, Zr, Ba, and Mn. Relative ratios of Si/Ca and Si/Fe were used in distinguishing an elemental signature of sediment collected from the north side of the Contact Fault (Shoupe Glacier terminal moraine) in comparison to that residing to the south of the Contact Fault (Columbia Glacier terminal moraine).

2.5 Bulk Sediment Magnetic Grain Size Analyses

The magnetic characteristics of sediment collected from Columbia and Shoupe Glaciers were determined by a comparison of relative magnetic grain size, a well-known proxy achieved by the ratio of Anhysteretic Remanent Magnetization as a function of susceptibility versus raw susceptibility (kARM/k). First, the sand size fraction (<63μm) of terminal moraine sediment was isolated through sieving and was packed into $1cm^3$ plastic cubes. Bulk susceptibility (k) was measured at 0.47 kHz on a Barlington MS2B, while Anhysteretic Remanent Magnetization (kARM) was imparted at 100 mT on a 2G

Enterprises cryogenic magnetometer. All measurements were acquired at Oregon State University's Paleo-and Environmental Magnetism Laboratory following (Hatfield, et al., 2013)(Tab. 3). The magnetic profile characterization of bulk sediment followed marine core magnetic characterization was achieved prior to this investigation by Dr. Joseph Stoner .

3. RESULTS

3.1 Marine Core Chronology

Our ^{14}C derived age model indicated that marine core EW0408-95JC is representative of a ~1.6 ky time frame of stratigraphic history since the time it was collected in 2004 (furthermore referred to as "present day") (Fig. 3). The calendar dates acquired were in chronological order with increasing depth downcore, with the exception of an irregular region between 477 cm and 995 cm in which multiple age reversals occurred (Tab. 2). We interpreted this turbidic section of the marine core to be a gravity flow that resulted from a sediment pulse driven by the onset of Columbia Glacier advance during the Little Ice Age (Koppes 2010). This rapid deposition of large quantities of sediment, as indicated by the marked increase in sedimentation rate at this time (Fig. 3d), resulted in an increase in turbidity that mixed the sediment interface and displaced lower lying, older foraminifera shells to the surface, and younger shells at the surface to greater depths. These high intensity gravity flows are distinctive mechanisms in long distance sediment transportation from glacial fjord depocenters to offshore shelves on centennial (advance/retreat) timescales. The magnitude of this offshore sediment signal is highest when produced by glaciers acting within a meltwater dominated isothermal regime:

precise characteristics of Columbia Glacier (Jaeger and Koppes 2016). Based on these factors, we chose to exclude these measurements from the age model calculation and instead extrapolated across the gravity flow to obtain a relative age of the material.

3.2 Marine Core Geochemistry

The geochemical properties of marine core material was tightly correlated with the previously determined magnetic profile, with a distinct shift occurring at ~0.9kya: a transition separating two marked phases in the core profile. Prior to ~0.9 kya, the marine core was dominated by material with low kARM/k values and high ratios of Si/Ca and Si/Fe. From ~0.9 kya to present day, the marine core was dominated by material with high kARM/k values and small ratios of Si/Ca and Si/Fe. Coupled with this pronounced change in magnetic and geochemical regimes was a change in parameter variability. Prior to ~0.9 kya, magnetic and geochemical parameters were highly variable, transitioning to lower variability in the latter section of the core, from ~0.9 kya to present day (Fig. 3a, 3b, 3c).

3.3 Bulk Sediment Geochemistry and Magnetic Properties

Elemental analysis of sediment collected from Columbia and Shoupe Glacier's terminal moraines indicated distinct variations in the lithologies of the different regions. Material collected from Columbia Glacier's terminal moraine, located south of the Contact Fault, had high kARM/k values and low ratios of Si/Ca. In contrary, sediment collected from the Shoupe Glacier terminal moraine contained material with low kARM/k values low ratios of Si/Ca, and Si/Fe (Tab. 4).

4 DISCUSSION

4.1 Marine Core Geochemistry and Magnetic Variation

The chronological variation in magnetic and geochemical properties implied that two distinct phases are represented in the ~1.6 ky of material within our marine core. The relative low ratios of kARM/k and high ratios of Si/Ca, and Si/Fe prior to ~0.9 kya, suggested a source of weakly magnetic, coarse-grained material enriched in Silica. At ~0.9kya, the shift in parameters suggested a change in basal lithology to one of stronger magnetic, fine grained material enriched in Calcium and Iron. This transition coincides impeccably with the known differentiated lithologies on either side of the Contact Fault. Metasedimentary and metavolcanic material making up the inboard Valdez group are classified by paramagnetic silicon enriched material, while the outboard Orca group consisting of sedimentary rocks coupled with mafic intrusions is classified by strongly magnetic, calcium and iron enriched material.

4.2 Marine Core Sediment Provenance

Sediment provenance within the core is established as being of Columbia Glacier origin based on: 1) the oceanographic sediment transport regime within PWS; 2) the locations of prehistorical glacial maximum extents throughout the PWS; and 3) the observed difference in magnetic and geochemical signatures of sediment collected *in situ* from Columbia and Shoupe glaciers terminal moraines. Within PWS, two prominent sources of sediment exist: allchthonous sediment discharged from the Cooper River and autochthonous sediment originating from Columbia Glacier. The Cooper River discharges a massive plume of suspended sediment exceeding all other Alaskan rivers by a factor of two

(Brabets, 1997). This sediment is transported from the mouth of the river entrained in the anticyclonic gyre created by the divergence of the Alaska Coastal Current (ACC) off the coast of Kayak Island and settled to the seabed, or is carried by the ACC through Hinchinbrook Entrance into PWS (Fig. 1). Sediment entrained and transported by the ACC is at the will of the currents high variability in seasonal geostrophic flow patterns. Marine core site EW0408-95JC lies directly in the path of the summer through fall cyclonic circulation patterns, the season in which glacial sediment discharge is at a maximum, driven by high freshwater discharge in the active ablation zone. Of the three glaciers that contribute sediment into this cyclonic seasonal circulation flow (Shoupe, Columbia, and Mears) (Fig. 2), evidence depicted in preserved maximum extent terminal moraines show that Columbia Glacier is the only one in the region that has advanced south across the Contact Fault in the last millennium (Molina, 2008). Thus, sediment in the core with mafic like magnetic and geochemical signatures is, by default, of Columbia Glacier provenance. Using this wealth of information in addition to direct measurements of sediment from either side of the Contact Fault provides evidence that the shift in geochemical and magnetic properties occurring downcore within EW0408-95JC is indeed depicting lithological changes of sediment eroded and discharged from Columbia Glacier.

4.3 Millennial Timescale Columbia Glacier Retreat

We conclude that at ~0.9 kya, Columbia Glacier advanced south across the Contact Fault and transitioned from eroding Valdez Group metasedimentary sandstones to eroding Orca group sandstones and intruded mafic basalts. We compared these findings to dendrochronology derived tree kill dates of hemlock forests (*Tsuga mertensiana)* overrun

by Columbia Glacier during its most recent advance. This record places Columbia Glacier advancing in 1020 CE to a mid-fjord stationary position in 1400 CE. It than began readvancing in ~1700 CE and reached its maximum extent as late as 1810 CE (Wiles, et. al.) These two synonymous records portray that Columbia Glacier advanced south across the Contact Fault at ~0.9 kya, consistent with various other findings of Southern Alaskan and Central Coastal Mountain Range late Holocene glacial expansion occurring ~1 kya (Barclay, 2009). However, the dendrochronology record doesn't constrain periods of potential ice margin retreat, which could be implied by the lengthy gap in kill dates between 1400-1700 C.E. (Wiles et. al 2014). Yet, we expect that an ice margin retreat would be depicted in the marine core as a decrease in kARM/k and an increase in Si/Ca and Si/Fe geochemical parameters coupled with an increase in sedimentation rate driven by glacial retreat (Jaeger and Koeeps, 2016). This predicted signature of retreat is readily evident in multicore EW0408-95MC, in which a decrease in kARM/k, increase in Si/Ca and Si/Fe occurred as the glacier approached the Contact Fault (Fig. 4). These findings mark Columbia Glacier in an extended position, beginning ~0.9 kya and maintaining this extended state until recent retreat ensued and resulted in retreat north across the fault in ~2002. Recent Columbia Glacier retreat is thus unprecedented with respect to a millennial timescale.

Based on the anomalous extent of recent retreat in comparison to retreat events over the last millennium, we argue that an external forcing was the driving factor in propagating an event of such a magnitude. As an isothermal, temperate tidewater glacier, the regime of Columbia Glacier is one of extensive winter season accumulation and summer melting. The two potential factors that could have an effect on glacial mass balance are thus a decrease in winter accumulation, or an increase in summer temperature. Winter season

accumulation at sea level of Columbia Glacier, extrapolated from the nearest weather station located in the area, has increased in the last century. Leaving the recent change in surface air temperature, a result of anthropogenic activities (Aerndt, 2009), as the sole climatic driver of glacial destabilization. We tested this hypothesis by analyzing prehistorical reconstructions and observed recent summer season temperature changes in the PWS to depict Columbia Glaciers sensitivity to specific surface air temperature profiles.

4.5 Surface Air Temperature Forcing on Retreat

A February through August Gulf of Alaska (GoA) temperature reconstruction suggests three main temperature phases in the last millennium. These include a warming centered around 950 C.E., a long term cooling with distinct phases centered around 1190, 1450,1650, and 1850 C.E., and finally a recent warming over the last century (Wiles, et al. 2004). The 950 C.E. warming phase coincides with our interpretation of the last time Columbia Glacier resided in a retreated position north of the Contact Fault and warming over the last century coincides with modern retreat to a position north of the Contact Fault. This suggested similar temperature profiles between prehistoric retreat and modern day retreat. Furthermore, a temperature reanalysis at 900mb, the approximated elevation of Columbia Glacier's equilibrium line altitude, suggested a contemporary warming over the last century with a 1.2 °C temperature increase from the 1870-1890 mean occurring when Columbia Glacier retreat was initiated (Colgan, 2012).

We tested the relative significance of this warming trend on the stability of Columbia Glacier using 3020 model simulations where the rate and magnitude of warming were varied in inducing glacial retreat. The total 1.2°C warming over 70 years (0.017 $°Ca^{-1}$)

agrees with the model simulations. Furthermore, the model simulated temperature destabilization of Columbia Glacier is 1.1 ± .2 °C, agreeing with the ambient surface air temperature when Columbia Glacier destabilized from its moraine shoal and rapid retreat ensued (Colgan, 2012) (Fig. 4). Coupling the prehistoric and modern day temperature profiles show that similar temperature profiles existed in both retreat initiated in 1978 and the most prior.

The similar surface air temperature profiles during recent and prehistoric retreat suggests temperature increase within PWS as a trigger of Columbia Glacier destabilization. These findings imply that climatic forcings may indeed have effects on tidewater glacier cycles on a long-term basis. Internal dynamics such as fjord geometry, glacial drainage basin, and ice flow velocity control glaciers response time and susceptibility to climatic change, however, when specific climatic thresholds are reached these internal dynamics may become second order forcings. Columbia Glacier was the last glacier in the PWS to begin advancing during the Little Ice Age period, and again was the last glacier in PWS to retreat from its Little Ice Age maximum extent (Barclay, 2009). Thus, internal dynamics seem to be inducing longer response times and lower susceptibility to climatic changes, yet a threshold temperature of 1.2°C induces Columbia Glacier retreat. These findings prove significant for our greater understanding of tidewater glaciers worldwide by increasing our understanding of tidewater glacier susceptibility to climatic forcings. This is a feat that is and will continue to be vital in the rapidly changing climatic state of the current Anthropocene era.

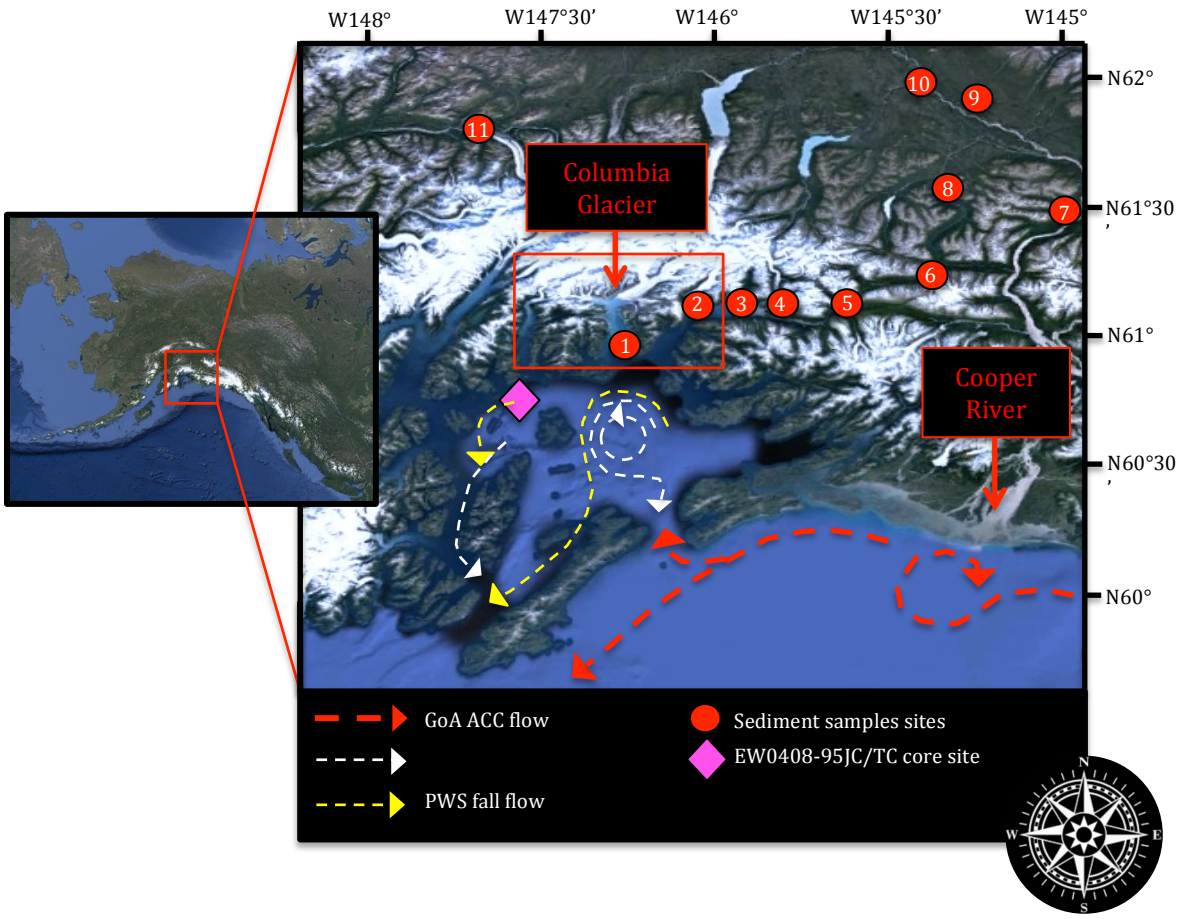

Figure 1. Location of study area within PWS and greater GoA. Red dashed line depicts the flow of the ACC current in the GoA with respect to the Cooper River sediment plume. White and yellow lines depict summer and fall season ACC geostrophic flow patterns. Purple diamond depicts location of marine core EW0408-95JC/TC/MC. Bulk sediment stream and terminal moraine sample locations depicted by circles 1-11.

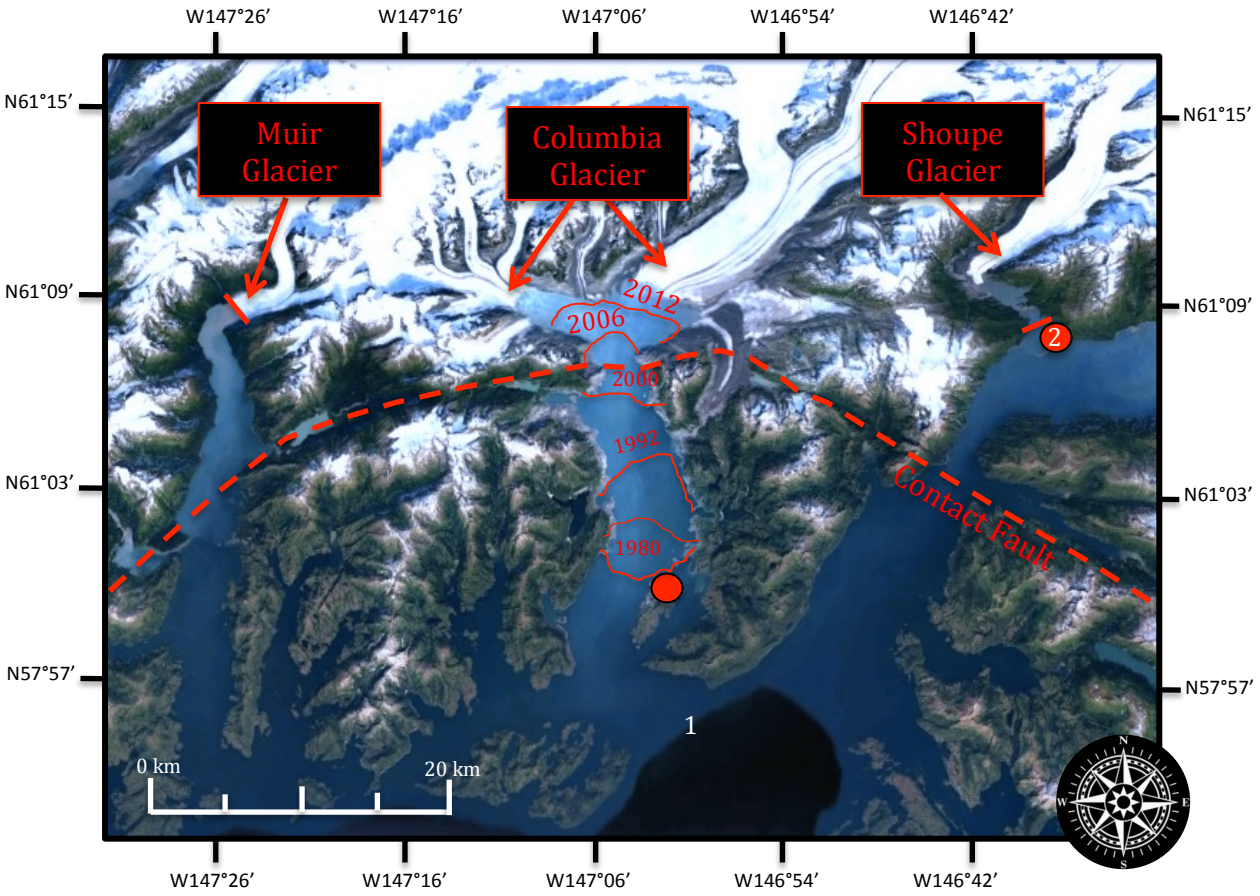

Figure. 2 Geographic location of Columbia Glacier including 6-year terminal ice margin extent from 1980 C.E. to 2010 C.E. (McNabb and Hock, 2014). Red dashed line shows location of the Contact Fault in the region. Maximum extents of Muir and Shoupe glacier in the last millennium (Molina 2008) shown by solid red lines. Bulk sediment sites 1 (Columbia Glacier terminal moraine & 2 (Shoupe Glacier terminal moraine)

Table 1. Geographic locations of 11 bulk sediment stream and terminal moraine samples obtained during June of 2015. Red is sediment samples used in analyses.

Sample	Location	Latitude	Longitude	Elevation
1	Columbia Glacier Terminal Moraine	61°59'49"N	147°1'49"W	0 m
2	Shoupe Glacier Terminal Moraine	61°6'59"N	146°35'13"W	0 m
3	Mineral Creek	61°8'1"N	146°23'19"W	14 m
4	Valdez Glacier Terminal Moraine	61°8'57"N	146°10'17"W	76 m
5	Worthington Glacier Terminal Moraine	61°10'2"N	145°43'41"W	775 m
6	Tiekel River Bank	61°14'3"N	145°21'43"W	386 m
7	Junction of Cooper River and Chitina River	61°31'12"N	144°25'1"W	146 m
8	Tonsina River Bank	61°3'56"N	145°11'19"W	442 m
9	Klutina River Bank	61°57'13"N	145°19'18"N	326 m
10	Tazlina River Bank	62°3'11"N	145°25'37"W	345 m
11	Matanuska Glacier Terminal Moraine	61°46'29"N	147°45'13"W	479 m

Table. 2. Radiocarbon measurements of discrete sediment samples used to derive our age model. Red is newly obtained measurements in this investigation, others were obtained prior by Leah Ziegler. Yellow shading (478-976 cm. below surface) depicts turbulent gravity flow section of core EW0408-95JC in which multiple age reversals occurred.

Core	Material	Depth in core (cm)	Depth below surface (cm)	^{14}C age	1 sigma	Calibrated age	1 sigma
EW0408-95TC	Benthic	5	11	650	60	Post-Bomb	Post-Bomb
EW0408-95JC	Benthic	1	77	1535	30	360	90
EW0408-95TC	Benthic	91	97	1830	50	600	80
EW0408-95JC	Benthic	101	178	1705	50	510	90
EW0408-95TC	Benthic	212	218	2110	45	850	110
EW0408-95JC	Benthic	201	278	2025	15	770	90
EW0408-95JC	Benthic	301	378	1935	20	690	90
EW0408-95JC	Benthic	401	478	2265	15	1010	110
EW0408-95JC	Benthic	751	828	4255	45	3310	140
EW0408-95JC	Benthic	780	857	1980	55	1070	100
EW0408-95JC	Planktonic	780	857	2320	30	1070	110
EW0408-95JC	Benthic	802	879	3195	20	2020	130
EW0408-95JC	Benthic	828	905	2375	35	1120	110
EW0408-95JC	Benthic	880	957	2370	35	1110	110
EW0408-95JC	Benthic	899	976	2355	20	1100	110
EW0408-95JC	Benthic	901	978	2625	15	1370	100
EW0408-95JC	Benthic	1298	1375	2665	40	1410	110
EW0408-95JC	Benthic	1720	1797	2880	20	1650	120

Table.3 Columbia and Shoup glacier terminal moraine bulk sediment magnetic grain size analysis results as a function of anhysteretic remnant magnetization (kARM) and bulk susceptibility (k).

Glacier	kARM	k	kARM/k
Columbia	.00005	.000055	.866
Shoup	.000626	.002623	3.35

Table. 4 Columbia and Shoup glacier terminal moraine bulk sediment geochemical analysis results

Glacier	Si (ppm)	Ca (ppm)	Fe (ppm)	Si/Ca	Si/Fe
Columbia	454	164	6412	2.77	.071
Shoup	471	362	11707	1.30	.040

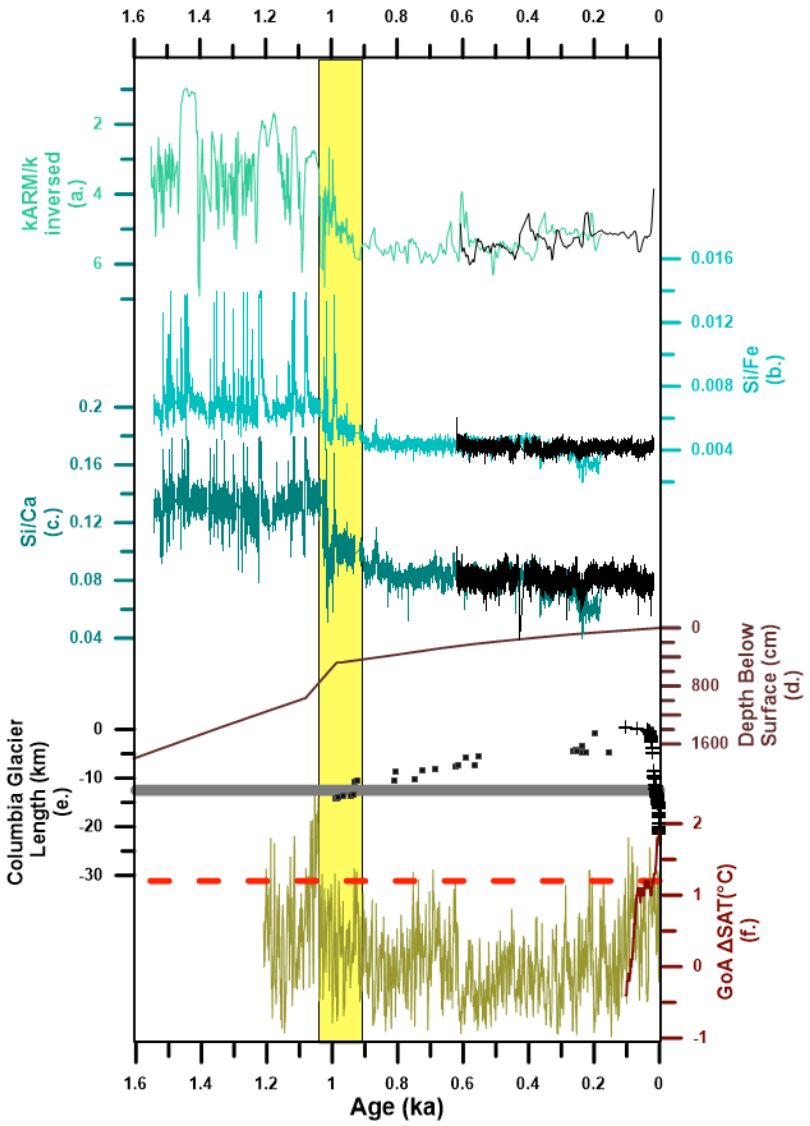

Figure 3. (a.) Inversed kARM/k of EW0408-95JC material. Increase in kARM/k indicative of fine grain (stronger) magnetic material, decrease in kARM/k indicative of coarse grain (stronger) magnetic material. **(b.)** Silica to Calcium ratio of EW0408-95JC material. **(c.)** Silica to Iron ratio of EW0408-95JC material. Black lines showing relative parameters of EW0408-95TC material. **(d.)** Relative depth below the ocean-sediment interface. Increase in rate resembles increase in sedimentation rate. **(e.)** Length of the Columbia Glacier with respect to modern day maximum extent. Squares represent lengths derived from tree kill dates, crosses represent observed lengths (Mcnabb and Hock, 2014). **(f.)** Gulf of Alaska surface air temperature derived from tree ring dendrochronology measurements (Wiles, et al., 2014). Solid red line represents temperature reanalysis at 900mb, the relative elevation of Columbia Glacier's equilibrium line altitude (Colgan, et. al., 2012). Yellow bar represents the age span of the gravity flow deposit. Dashed red line is surface air temperature during onset of Columbia Glacier retreat.

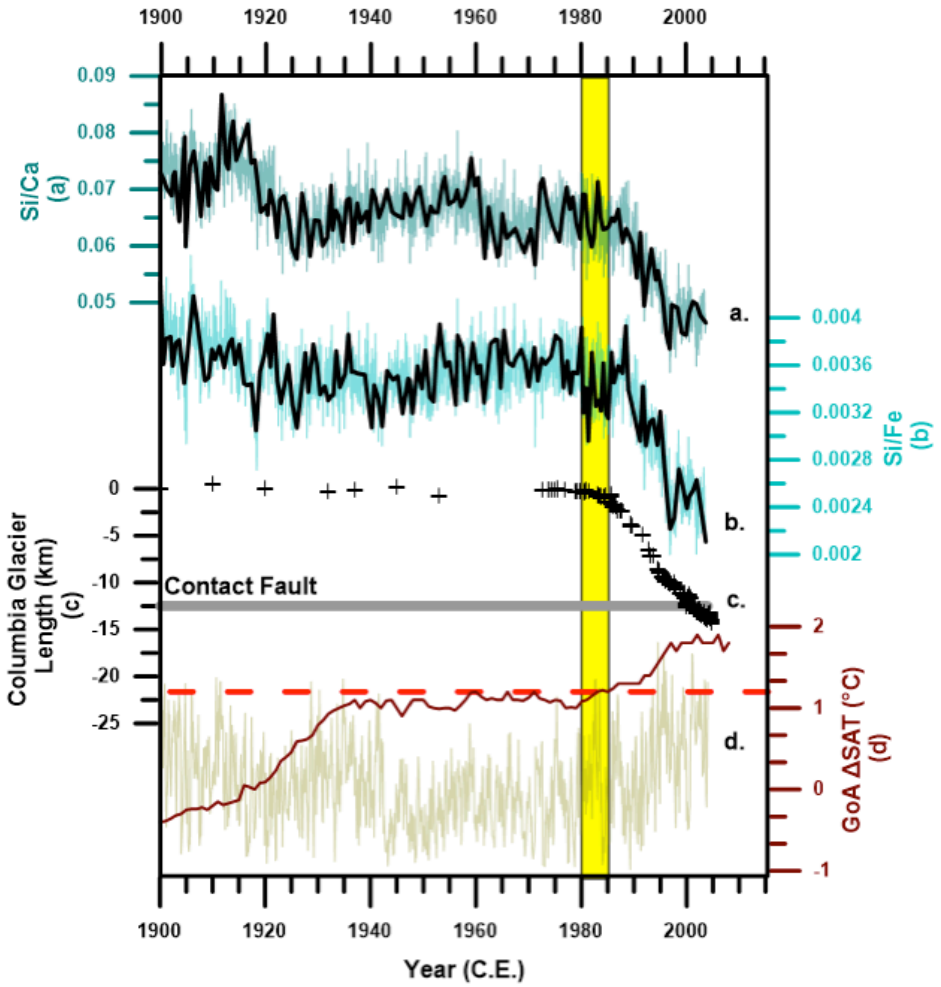

Figure 4. (a) Silica to Calcium ratio of material within marine core EW0408-95MC. **(b)** Silica to Iron ratio of material within marine core EW0408-95MC. **(c)** Observed changes in Columbia Glacier length from the 1978 stable equilibrium position (McNabb and Hock, 2014). The Contact Fault is distinguished as horizontal grey line. **(d.)** Surface air temperature profile from Figure 2. Red dashed line represents temperature profile at time of Columbia Glacier retreat. Yellow vertical bar represents time of Columbia Glacier retreat.

REFERENCES

Arendt, A., Walsh, J., and Harrison, W., 2009, Changes of glaciers and climate in Northwestern North America during the late twentieth century: Journal of Climate, v. 22, p. 4117-4134.

Barclay, D.J., Wiles, G.C., and Calkin, P.E., 2009, Holocene glacier fluctuations in Alaska: Quaternary Science Reviews, v. 28, p. 2034-2048.

Berthier, E., Schiefer, E., Clarke, G.K.C., Menounos, B., and Rémy, F., 2010, Contribution of Alaskan glaciers to sea-level rise derived from satellite imagery: Nature Geoscience, v. 3, p. 92-95.

Brabets, T., 1996. Geomorphology of the lower Copper River, Alaska. United States Geological Survey Professional Paper 1581.

Colgan, W., Pfeffer, W.T., Hajaram, H., Abdalati, W., and Balog, J., 2012, Monte Carlo ice flow modeling projects a new stable configuration for Columbia Glacier, Alaska, c. 2020: The Cryosphere, v. 6, p. 1395-1409.

Davies-Walczak, M., Mix, A.C, Stoner, J.S., Southon, J.R., Cheseby, M., Xuan, C., 2014, Late Glacial to Holocene radiocarbon constrains on North Pacific Intermediate Water ventilation and deglacial atmospheric CO2 sources: Earth and Planetary Science Letters, v.397, p.57-66

Hill, D.F., Ciavola, S.J., Etherington, L., Klaar, M.J., 2009, Estimation of freshwater runoff into Glacier Bay, Alaska and incorporation into a tidal circulation model: Estuarine, Coastal, and Shelf Science, v.82, p.95-107

Hatfield, R.G., Stoner, J.S., Carlson, A.E., Reyes, A.V., Housen, B.A., 2013, Source as a controlling factor on the quality and interpretation of sediment magnetic records from the northern North Atlantic: Earth and Planetary Science Letters, v.368, p.69-77

Jaeger, J.M., and Koppes, M.N., 2016, The role of the cryosphere in source-to-sink systems: Earth-Science Reviews, v. 153, p. 43-76.

McNabb, R.W., and Hock, R., 2014, Alaska tidewater glacier terminus positions, 1948-2012: Journal of Geophysical Research, v. 119

McNeely, R., Dyke, A.S., Southon, J.R., 2006, Canadian marine reservoir ages, preliminary data assessment: Geologic Survey of Canada, Open File 5049, p.3

Meier, M.F., 1987, Fast Tidewater Glaciers: Journal of Geophysical Research, v. 92, p. 9051-9058.

Miller, E., 2014, High-resolution records of seismicity and seasonal sedimentation from Prince William Sound, Alaska, using XRF core scanning [MS. Thesis]

Molnia, B.F., 2008, Glaciers of North America – Glaciers of Alaska: U.S.G.S. Professional Paper 1386-k.

Musgrave, D.L., Halverson, M.J., and Pegau, W.S., 2013, Seasonal surface circulation, temperature, and salinity in Prince William Sound, Alaska: Continental Shelf Research, v. 53, p. 20-29.

Nick, F.M., van der Veen, C.J., and Oerlemans, J., 2007, Controls on advance of tidewater glaciers: Results from numerical modeling applied to Columbia Glacier: Journal of Geophysical Research, v. 112

O'Neel, S., Pfeffer, W.T., 2005, Evolving force balance at Columbia Glacier, Alaska, during its rapid retreat: Journal of Geophysical Research, v. 110

O'Neel and 13 others, 2015, Icefield-to-ocean linkages across the northern Pacific coastal temperate rainforest ecosystem: Bioscience, v.65, p.499-512

Post, A., O'Neel, S., Motyka, R.J., and Streveler, G., 2011, A complex relationship between calving glaciers and climate: Eos, v. 92, 305-312.

Sakakibara, D., Sugiyama, S., 2014, Ice-front variations and speed changes of calving glaciers in the southern Patagonia icefield from 1984-2011

Wiles, G.C., D'Arrigo, R.D., Barclay, D., Wilson, R.S., Jarvis, S.K., Vargo, L., and Frank, D., 2014, Surface air temperature variability reconstructed with tree rings for the Gulf of Alaska over the past 1200 years: The Holocene, v. 24, 198-208.

Wilson, F.H., and Hults, C.P., 2012, Geology of the Prince William Sound and Kenai Peninsula Region, Alaska: U.S.G.S. Scientific Investigation Map 3110.

Winkler, G., 2000. A geological guide to Wrangell-Saint Elias National Park and Preserve, Alaska: a tectonic collage of northbound terranes. United States Geological Survey Professional Paper 1616.